

The N/Z dependence of the nuclear caloric curve

S. Wuenschel, A. Bonasera, S. J. Yennello, G. A. Souliotis, D. V. Shetty,
S. N. Soisson, B. C. Stein, Z. Kohley, and L. W. May

Projectile fragmentation sources were identified from reactions of $^{86,78}\text{Kr}+^{64,58}\text{Ni}$ at 35 MeV/A collected with the upgraded NIMROD-ISiS array[1,2]. This data has been calibrated, particle identified, and analyzed to isolate the quasi-projectile source[3].

This source has been isolated using four data cuts. The first data cut was a minimum sum of charge detected in an event (sumZ) of 30 or greater. This cut was followed by a velocity cut [4] placed on the individual fragments to remove pre-equilibrium and target sources from the data. The third cut was a sumZ range of 30-34 to ensure that a consistent size of source is being studied. The final cut was based on the event shape and allowed only fairly spherical events to be retained. The source defined in this manner was then assigned an excitation energy from (1) where the sum is over the kinetic energy of the event fragments in the reconstructed frame of the event. The multiplicity of neutrons (M_n) was obtained from (2).

$$E^* = \sum_i^{Mcp} KE_i + M_n \langle KE_n \rangle - Q \quad (1)$$

$$M_{QP} = \frac{M_{\text{exp}} - M_{\text{bkg}}}{\left(\text{Eff}_{QP} + \frac{N_T}{N_P} \text{Eff}_{QT} \right) \left(\frac{.7}{.6} \right)} \quad (2)$$

Using Eq. (2), the multiplicity of neutrons was corrected on an event-by-event basis for background ($M_{\text{exp}} - M_{\text{bkg}}$). The number of neutrons assigned to the quasi-projectile source was then calculated with source tagged neutrons from the HIPSE-SIMON [5] event generator coupled to a GEANT-3 [6] simulation of the Neutron Ball. The Neutron Ball efficiency for quasi-projectile neutrons (Eff_{QP}) and quasi-target neutrons (Eff_{QT}) was included as well as the target and projectile neutron numbers (N_T and N_P). A final correction factor was added because the neutron ball was calibrated to 70% efficiency while the simulation yields an overall 60% efficiency.

A new thermometer has been derived from the momentum quadrupole fluctuations of fragments in the source frame. For each fragment in an event the fluctuations can be defined as $Q_i = 2P_z^2 - P_y^2 - P_x^2$. The distribution of Q_i across a class of events provides a variance that is linked to the temperature through (3).

$$\sigma^2 = 12m_0^2 T^2 \sum_i (\zeta_i A_i) \quad (3)$$

The beam (Z) axis was found to have residual collective behavior. This caused the derived fluctuation thermometer to provide temperature measurements dependent on the axis defined with the factor of 2. The thermometer was re-derived using only the transverse momentum to avoid this collective behavior. In this case $Q_i = P_x^2 - P_y^2$ is linked to the source temperature through (4).

$$\sigma^2 = 4m_0^2 T^2 \sum_i (\zeta_i A_i) \quad (4)$$

The temperature obtained from this thermometer has been found to be fragment mass dependent. This dependence may be the result of Coulomb repulsion, fragment recoil during break up, or Fermi momentum of the nucleons in the fragments [7,8]. The Fermi momentum is only a viable concern for $A \geq 2$ fragments. This thermometer may be used for protons without contamination from Fermi momentum or concern about fragment recoil. In addition the effect of Coulomb will be relatively small compared to the more massive fragments.

Fig. 1 shows the caloric curve derived from the proton momentum fluctuations for the more

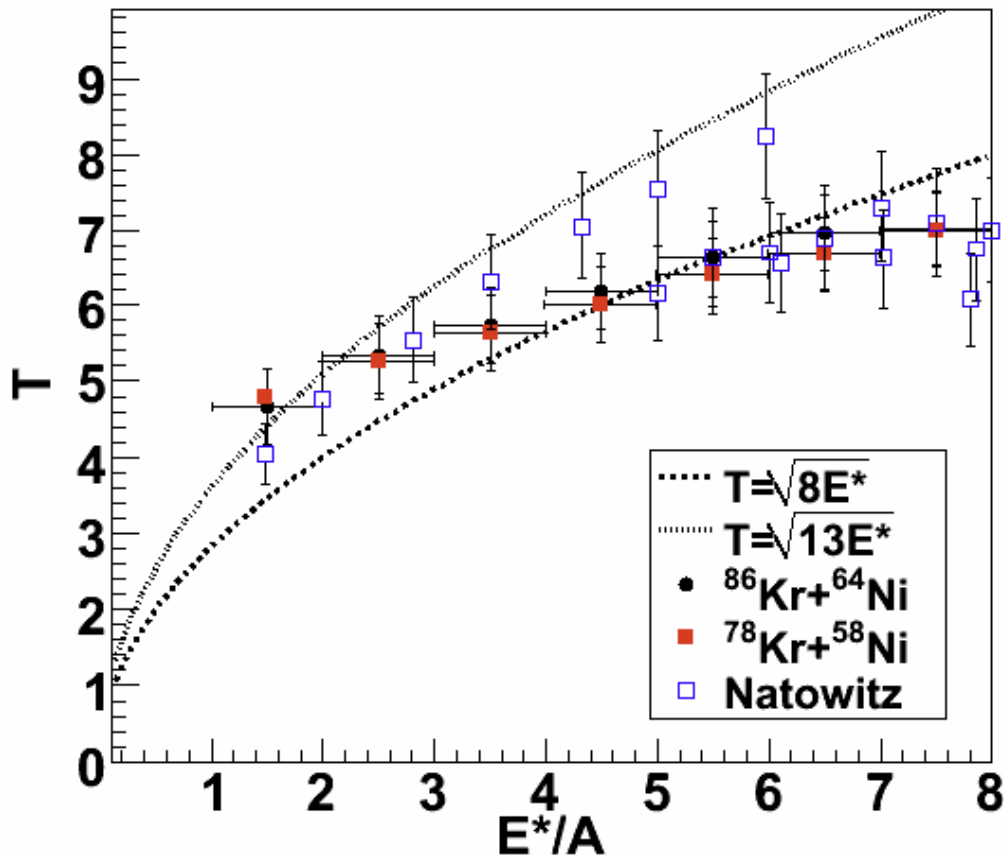


FIG. 1. Caloric curve derived from the transverse momentum fluctuations of protons with Natowitz compilation for reference [9].

neutron rich $^{86}\text{Kr}+^{64}\text{Ni}$ source and the less neutron rich $^{78}\text{Kr}+^{58}\text{Ni}$ source. These curves are plotted with two Fermi Gas curves for reference. An additional reference point is provided by the compilation of Natowitz *et al.* [9] from experimental measurements on similarly sized sources.

The momentum fluctuation thermometer agrees with the Fermi Gas ($T = \sqrt{aE^*}$, $a=8,13$) predictions at low excitation energy. In addition, at higher excitation energies, it flattens though it does not yield a completely flat plateau.

The two sources depicted in Fig. 1 yield temperatures that are nearly identical and are well within errors of each other. This thermometer does not exhibit a significant source N/Z dependence.

- [1] S. Wuenschel *et al.*, *Progress in Research*, Cyclotron Institute, Texas A&M University (2006-2007), p II-34.
- [2] S. Wuenschel *et al.*, *Nucl. Instrum. Methods Phys. Rev.* **A604**, 578 (2009).
- [3] S. Wuenschel *et al.*, *Progress in Research*, Cyclotron Institute, Texas A&M University (2007-2008), p II-28.
- [4] J. Steckmeyer *et al.*, *Nucl. Phys.* **A686**, 537 (2001).
- [5] D. Lacroix, A. V. Lauwe, and D. Durand, *Phys. Rev. C* **69**, 054604 (2004).
- [6] GEANT <http://wwwasd.web.cern.ch/wwwasd/geant/>.
- [7] S. Wuenschel, Ph. D. Thesis, Texas A&M University (2009).
- [8] W. Bauer, *Phys. Rev. C* **51**, 803 (1995).
- [9] J. B. Natowitz *et al.*, *Phys. Rev. C* **65**, 034618 (2002).